

Final-state interaction and intersubband spectroscopy in silicon inversion layers

S. Das Sarma

Department of Physics and Astronomy, University of Maryland, College Park, Maryland 20742

R. K. Kalia

Argonne National Laboratory, Argonne, Illinois 60439

M. Nakayama

Kyushu University, Fukuoka, Japan

J. J. Quinn

Brown University, Providence, Rhode Island 02912

(Received 18 May 1981)

We have investigated the effect of "ladder-bubble" vertex correction on the polarizability function for the transitions between the ground and excited subbands in a (100) Si-SiO₂ surface inversion layer. At all inversion layer concentrations we find a large cancellation between the dynamical vertex* correction and the resonance screening effect. Calculations for the resonance energies are close to the subband separations that include exchange-correlation effects and agree well with the spectroscopic measurements.

I. INTRODUCTION

In a metal-oxide-semiconductor (MOS) system, the presence of an electric field normal to the interface confines the electrons and quantizes their motion into electric subbands. There are two sets of such quantized levels in a (100) Si-SiO₂ surface inversion layer; (1) a twofold-degenerate set (0,1,2, . . .) associated with the heavier electron mass (≈ 0.9) perpendicular to the plane of the inversion layer, and (2) a fourfold-degenerate set (0',1',2', . . .) associated with the lighter mass (≈ 0.2).¹ Comparison with spectroscopic measurements show that the Hartree calculation² for the subband structure is inadequate and that the absorption energies are quite close to the differences in the quasiparticle energies which include exchange and correlation.³⁻⁸ However, it is misleading to relate the energies of observed absorption peaks to the subband separation because the spectroscopic measurements are always accompanied by two physical effects which must be included in a calculation before comparing it with the experiment. One of these effects, known as the resonance screening (depolarization shift), is caused by the screening of the incident light by the inversion layer electrons.^{4,9-12} Calculation of depolarization shift is straightforward, and it is found to increase the observed resonance absorption energies above the subband separations.

The second effect, known as the vertex correction (final-state interaction or excitonlike shift), is due to the interaction between an electron in an excited subband and the hole in the ground subband. In this paper we investigate the effect of final-state interaction on intersubband transition (given by the peaks in the corresponding polarizability, or equivalently, in the conductivity for the long wavelength limit) by including vertex corrections in the theory. This is done by including all the "ladder-bubble" diagrams containing the repeated interaction between the electron and the hole in the polarizability in an approximate fashion, in addition to the lowest-order intersubband polarizability bubble. The lowest-order polarizability has a pole at the quasiparticle energy difference between the two subbands. But the vertex correction through the ladder-bubble series shifts the pole to lower energy so as to partially cancel the depolarization shift. The cancellation occurs for all transitions (0 \rightarrow 1;0 \rightarrow 2) and inversion layer concentrations ($N_{\text{inv}} = 10^{11} - 3 \times 10^{12} \text{ cm}^{-2}$) that we have investigated. The resonance energies including these two effects are, therefore, close to the corresponding quasiparticle energy differences and to the experimental values. In Sec. II we discuss the theory explaining the basis set used for the calculation, as well as the approximation scheme in which the dynamical ladder-bubble diagrams were included. In Sec. III we discuss the results, comparing in

particular with Ando's calculation¹² of final-state interaction. We conclude in Sec. IV with a discussion of what we believe to be the status of the field.

II. THEORY

We are interested in evaluating the polarizability diagrams at zero temperature. However, we shall first formulate the problem at finite temperature and subsequently take the quantum limit. At a finite temperature we approximate a quasiparticle propagator by¹³

$$G_{ij}(\vec{p}; z) = \delta_{ij} \left[z - \left[E_i^* + \frac{p^2}{2m_i} - \mu \right] \right]^{-1}, \quad (1)$$

where \vec{p} defines the particle momentum in the plane of the inversion layer, μ the chemical potential of the system, and z a complex frequency. In Eq. (1) E_i^* , the energy associated with the bottom of the i th subband, is a sum of the Hartree and the exchange-correlation self-energy.^{4,5,14} We take $\hbar=1$ throughout.

E_i^* is calculated in the recently developed many-body—density-functional technique.¹⁵ In this new method¹⁵ the Hartree potential is modified by adding to it a term V_{xc} which approximates the effect of exchange and correlation and contains a parameter B . The variational solutions of the modified Schrödinger equation (including V_{xc}) provide the basis set for the calculation of subband self-energies. The contribution of the additional term is subtracted from the electron-electron interaction to give H' , the perturbation used in evaluating the self-energies. The parameter

B is varied until the self-energy of the ground subband vanishes. With the new perturbation, the self-energy of an excited subband is found to be much smaller than the corresponding Hartree energy. In a (100) silicon inversion layer the energy separation between the ground and the first excited subband is found to be very close to the value reported in earlier perturbation calculations.¹⁴ Furthermore, the parameter B in the exchange-correlation potential is found to be essentially independent of the inversion layer concentration. One advantage of this new technique is that the one-electron basis set $\{\xi_i(z)\}$ so obtained includes some effects of electron-electron interaction in the sense of density-functional method.¹² For details of this many-body—density-functional technique we refer to Ref. 15.

From the form of the propagator, it is apparent that the quasiparticles are assumed to be extremely long lived. The reason for neglecting the lifetime effects is a practical one, for the calculation of polarizability becomes extremely difficult with finite lifetime effects. In Eq. (1) we have also assumed that the quasiparticle energy dispersion is the same as that for the free particles. This is quite a reasonable approximation, because in the calculation of polarizability, most of the contribution comes from $k \leq 2k_F$ (where k_F is the 2D Fermi wave vector) and in this range the self-energies are almost independent of wave vector k .^{4,14} Finally, the particle propagator in Eq. (1) is taken to be diagonal in the subband indices. The reason for the diagonal approximation will be explained later.

With quasiparticle propagators, the lowest-order contribution to the polarizability function can be written¹³

$$\Pi_{ij}(\vec{q}; i\nu_m) = \frac{1}{\beta} \sum_{\vec{k}} \sum_{\omega_n} G_{ii}(\vec{k} - \vec{q}; i\omega_n - i\nu_m) G_{jj}(\vec{k}; i\omega_n), \quad (2)$$

where $\beta = 1/k_B T$, $\omega_n = (2n+1)\pi/\beta$, $\nu_m = 2m\pi/\beta$ (m and n are integers), and the summation over \vec{k} includes the spin and valley degeneracies.

By substituting Eq. (1) into Eq. (2) and performing the frequency sum over ω_n ,¹³ we find that in the quantum limit the vertical transition ($\vec{q}=0$) between the ground ($i=0$) and an excited subband is described by

$$\Pi_{0j}^{(1)}(0; i\nu_m = \Omega) = \frac{N_S}{(\Omega - E_{j0}^*)}, \quad (3)$$

where $E_{j0}^* = E_j^* - E_0^*$, and N_S is the inversion layer density. For the vertical transition the contribution to the polarizability from the first-order vertex term can be written¹³

$$\Pi_{ij}^{(2)}(0; i\nu_m) = \frac{-1}{\beta^2} \sum_{\vec{q}, \vec{q}'} \sum_{\omega_n, \nu_l} G_i(\vec{q} + \vec{q}'/2; i\omega_n - i\nu_m) G_i(\vec{q} - \vec{q}'/2; i\omega_n - i\nu_l - i\nu_m) \\ \times U_{ij}(\vec{q}'; \nu_l) G_j(\vec{q} - \vec{q}'/2; i\omega_n - i\nu_l) G_j(\vec{q} + \vec{q}'/2; i\omega_n), \quad (4)$$

where $G_i \equiv G_{ii}$ and U_{ij} is the screened Coulomb interaction. In fact U_{ij} stands for U_{ijjj} . According to Dyson's equation, U_{ijlm} is proportional to V_{ijlm} —the sum of the bare Coulomb and the image interactions.^{4,14} Explicit calculations¹⁴ reveal that V_{ijlm} and consequently U_{ijlm} are small unless $i=j$ and $l=m$. Under these conditions, the self-energies and the Green's functions [Eq. (1)] become diagonal in the subband indices within the lowest-order screening approximation.¹⁴ We make the plasmon-pole approximation¹⁴ for the screened interaction in Eq. (4). The usefulness of the plasmon-pole approximation has been stressed in

the 3D electron gas^{16,17} and it has also been successful in explaining the quasiparticle properties in inversion layers.^{4,14} Performing the frequency sums over ω_n and ν_l in Eq. (4) and then going over to the quantum limit we find (in the reduced units),

$$\Pi_{0j}^{(2)}(0; \Omega) = - \frac{C_j(\Omega)}{(\Omega - E_{j0}^*)^2} \frac{1}{(e^2 a^*)}, \quad (5)$$

where the length is measured in units of $a^* = \hbar^2 / m_{11} e^2$ (m_{11} is the electron mass in the plane of the inversion layer) and the energy in units of $e^2 / 2a^*$. The expression for $C_j(\Omega)$ can be written

$$C_j(\Omega) = \frac{4}{\pi^3} \left[\int_0^\infty dq' \bar{V}_{0j}(q') S_0(q') + \int_0^\infty dq' \bar{\omega}(q') \tau_{0j}(q') [S_1(q') + S_2(q'; E_{j0}^*) - S_2(q'; \Omega)] \right]. \quad (6)$$

The quantities S_0 , S_1 , and S_2 are given by

$$S_0(q') = \frac{1}{2} \int d^2q H(-\omega_0^*(\bar{q} + \bar{q}'/2)) H(-\omega_0^*(\bar{q} - \bar{q}'/2)), \quad (7)$$

$$S_1(q') = -\frac{1}{2} \int d^2q H(-\omega_0^*(\bar{q} + \bar{q}'/2)) H(-\omega_0^*(\bar{q} - \bar{q}'/2)) [\bar{\omega}(q') - 2\bar{q} \cdot \bar{q}']^{-1}, \quad (8)$$

and

$$S_2(q'; \Omega) = \frac{1}{2} \int d^2q H(-\omega_0^*(\bar{q} + \bar{q}'/2)) [-\Omega + E_{j0}^* + \bar{\omega}(q') - 2\bar{q} \cdot \bar{q}']^{-1}, \quad (9)$$

where

$$\omega_0^*(\bar{q}) = E_0^* - \mu + q^2. \quad (10)$$

In these equations $H(x)$ denotes a Heaviside function and $\bar{V}(\bar{q}) = qV(\bar{q})/e^2 a^*$. The integrals in Eqs. (7)–(9) are evaluated analytically, whereas those in Eq. (6) are performed numerically. The functions $\bar{\omega}(q)$ and $\tau_{0j}(q)$ are, respectively, the effective plasma frequency and the interaction strength in the plasmon-pole approximation.¹⁴ These are determined by using the f sum rule and Kramers-Kronig relations as explained in detail in Ref. 14.

The second-order polarizability $\Pi_{0j}^{(2)}(0; \Omega)$ turns out to be of the same order of magnitude as the lowest-order diagram $\Pi_{0j}^{(1)}(0; \Omega)$. This makes it imperative that the whole ladder-bubble series is taken into account in obtaining the intersubband transition frequencies. Inclusion of the whole ladder-bubble series in the polarizability is also consistent with our use of the self-consistent random-phase approximation (RPA) energies and wave functions to describe the quasiparticles in the subbands. An exact evaluation of all the ladder-

bubble diagrams is of course impossible in the system under consideration. So we have used the following approximate formula¹⁸ for the irreducible polarizability containing the lowest-order bubble ($\Pi_{0j}^{(1)}$) and the whole ladder-bubble series:

$$\Pi_{0j}(\Omega) \cong \Pi_{0j}^{(1)}(0, \Omega) / [1 - \Pi_{0j}^{(2)}(0; \Omega) / \Pi_{0j}^{(1)}(0; \Omega)]. \quad (11)$$

Equation (11) is known¹⁸ to reproduce the first three diagrams in the ladder-bubble series exactly. In addition Eq. (11) is exact for a short-range delta-function interaction. It is expected to yield reasonably good results even in the presence of dynamically screened vertex correction since the interaction is of sufficiently short spatial range. Note that Eq. (11) indicates that the pole of the polarizability shifts from $\Omega = E_{j0}^*$ to $\Omega = E_{j0}^* - C_j(\Omega)/N_s$ due to vertex correction. This result would not come out of any finite-order perturbation expansion. The irreducible polarizability $\Pi_{0j}(\Omega)$ given by Eq. (11) is used to form the total or the reducible response function $\chi_{0j}(\Omega)$, which can be written as⁴

$$\chi_{0j}(\Omega) = [\Pi_{0j}(\Omega) + \Pi_{0j}(-\Omega)] / \{ 1 - V_{0j0j}[\Pi_{0j}(\Omega) + \Pi_{0j}(-\Omega)] \}. \quad (12)$$

In Eq. (12), V_{0j0j} stands for

$$V_{0j0j} = \frac{4\pi e^2 a^*}{\kappa_s} \int_0^\infty dz \left[\int_0^z dz' \xi_0(z') \xi_j(z') \right]^2, \quad (13)$$

where κ_s is the semiconductor dielectric constant, and ξ_0, ξ_j are the wave functions (including exchange-correlation effects)¹⁵ of the ground and excited subbands.

The peaks of $\text{Im}\chi$ give the resonance absorption energies including the depolarization shift and the vertex correction. Neglecting vertex correction (i.e., $C_j=0$), $\text{Im}\chi_{0j}(\Omega)$ has a delta-function peak at $\Omega = [E_{j0}^*(E_{j0} + 2V_{0j0j}N_s)]^{1/2}$, which is the depolarization shifted result.

We investigate the peaks in $\text{Im}\chi_{0j}(\Omega)$ for $j=1,2$ numerically in the range of inversion layer density $N_s = 1 \times 10^{11} - 1.5 \times 10^{12} \text{ cm}^{-2}$. Results are given in the next section.

III. RESULTS

In Fig. 1 we display the resonance energies for the $0 \rightarrow 1$ transition as a function of inversion layer concentration, as given by the peaks of $\text{Im}\chi$. The quasiparticle energies and wave functions are those obtained by the many-body—density-functional technique. We find that the vertex correction tends to cancel a large part of the depolarization shift. The final resonance absorption energies (curve 4) are thus close to the corresponding quasiparticle energy differences (curve 1). This large degree of cancellation holds for transitions between $0 \rightarrow 1$ and $0 \rightarrow 2$ subbands at all concentrations.

Ando has earlier investigated¹² the effect of vertex correction on the subband structure by calculating the excitonlike shift using the density-functional method. His results agree well with experimental measurements. His final results are very similar to ours (compare curves 3 and 4 in Fig. 1), but the objection of using a static theory like the density-functional technique to study dynamic response of rather high frequencies makes his theory somewhat unjustifiable from fundamental principle. We would like to add, however, that the time-dependent—local-density approach used¹² by Ando has been quite successful in atomic physics.¹⁹ The fact that our result is quite close to Ando's lends some fundamental justification to the time-

dependent—local-density approach in calculating dynamical response. Ando also uses the static exchange-correlation potential corresponding to the ground state of the system to study the dynamic response. Because the energies of the excited states are considerably larger than the Fermi energy of the system, there is no reason to expect the static exchange-correlation potential to give quantitatively accurate results. When we use a statically screened vertex in our theory [i.e., we use the static screening in the interaction U_{ij} in Eq. (4)], we get a result²⁰ which is formally the same as Ando's. In the presence of dynamic screening, however, it is not possible to extract any such formal similarity analytically. For the sake of comparison we show the results of Ando's vertex correction¹² in Fig. 1 (curve 3) as against the dynamical vertex correction (curve 4) carried out in this work. We have used the same wave functions $\{\xi_i(z)\}$ and energies $\{E_i^*\}$ (calculated according to Ref. 15) to obtain both of these curves. To obtain curve 3 we use the

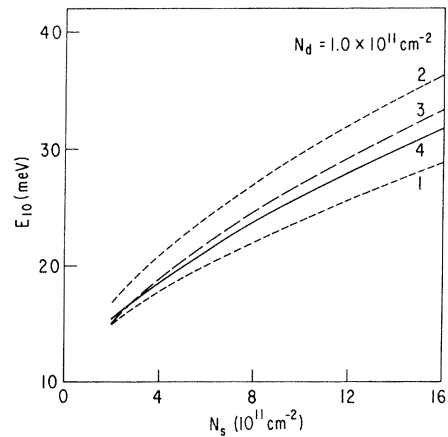


FIG. 1. Density (N_s) dependence of energy separation (E_{10}) between the ground subband 0 and the first excited subband 1 in a (100) Si-SiO₂ inversion layer. Curve 1 shows the quasiparticle energy difference between 0 and 1; curve 2 includes the depolarization shift; curve 3 takes into account the depolarization shift and the final-state interaction effect calculated by Ando's method, whereas curve 4 includes the depolarization shift and the dynamically screened final-state interaction effect. A calculation of vertex correction using the statically screened interaction (Refs. 4 and 20) would give a curve very close (≤ 1 meV below) to curve 2. N_{dep} has been taken to be $1.0 \times 10^{11} \text{ cm}^{-2}$.

prescription given by Ando in Ref. 12, whereas curve 4 is obtained by the method outlined in Sec. III. The point to note here is that the result (curve 4) with the dynamical vertex correction is even closer to the original quasiparticle energy difference (curve 1) than the result with Ando's density-functional-perturbational—final-state interaction. Thus the cancellation between depolarization shift and final-state interaction is even more complete when dynamically screened vertex correction is employed in the theory. Both Ando's and our results are close to experimental⁸ values of intersubband absorption energies. Also shown in the figure is the result with depolarization shift alone (curve 2) without any vertex correction.

IV. CONCLUSION

In conclusion, we have used many-body perturbation theory to evaluate the resonance position as observed in the infrared absorption measurements in Si(100)/SiO₂ inversion layers. The calculation includes self-energy, depolarization shift, and a dynamically screened vertex correction in a consistent fashion and is in good agreement with the experiment.⁸ We would like to emphasize the importance of dynamic screening in vertex correction—a fact that is not appreciated in the previous calculations. Since the self-energies are evaluated with dynamical screening, it is only consistent to treat the vertex correction in the same fashion.

It is, however, appropriate to insert a word of caution at this stage. There have essentially been three different calculations of final-state interaction effect in silicon inversion layers, namely the present calculation involving dynamical vertex correction through the ladder-bubble diagrams, Ando's calculation¹² employing density-functional-perturbational treatment, and Vinter's calculation⁴ where excitonic binding energy between the excited electron in the first subband and the hole left behind in the ground subband was obtained within a statically screened intersubband interaction. This last calculation is in fact equivalent to summing the ladder-bubble series for the vertex correction

using a static interaction,²⁰ rather than the fully dynamical interaction used in the present paper. The result^{20,4} of this statically screened vertex correction [by considering the statically screened U_{ij} in Eq. (4)] is a rather small (less than 1 meV) final-state interaction effect. On the other hand, the dynamically screened vertex correction could be quite large (~ 5 meV) as seen by comparing curves 2 and 4 in Fig. 1. Ando's calculation¹² which also employs a static interaction (but defined rather differently through the density-functional formalism) gives large vertex correction as well. The fact that dynamically screened vertex correction is larger than the static one can be understood easily on the basis of static screening being much stronger than dynamic screening on the average. Our present calculation confirms the general belief that the final-state interaction and the depolarization shift effects tend to oppose each other. The degree of cancellation between the two clearly depends on the approximation used. The ladder-bubble series while being expected to be the dominant set of diagrams for the excitonlike final-state interaction effect considered in this paper are by no means the only vertex diagrams for the problem. Other diagrams in each order are being left out. Thus from a theoretical viewpoint, the role of final-state interaction is by no means clear in a quantitative fashion. It would be interesting to have the subband energy differences directly by some experimental technique.¹² Since depolarization shift is accepted to be a quantitatively important effect, a precise experimental knowledge of subband energy difference will throw much light on the quantitative importance of the final-state interaction effect.

ACKNOWLEDGMENTS

The work was supported in part by the NSF, by the Materials Research Program at Brown University funded through the NSF, and by the ONR. The work of one of the authors (S. D. S.) at the University of Maryland is supported by NSF Grant No. DMR 7908819.

¹F. Stern and W. E. Howard, *Phys. Rev.* **163**, 816 (1967).

²F. Stern, *Phys. Rev. B* **5**, 4891 (1972).

³T. Ando, *Phys. Rev. B* **13**, 3468 (1976).

⁴B. Vinter, *Phys. Rev. B* **15**, 3947 (1977).

⁵F. J. Ohkawa, Ph.D thesis, University of Tokyo, 1975, unpublished.

⁶A. Kamgar, P. Kneschaurek, and G. Dorda, *Phys. Rev. Lett.* **32**, 1251 (1974).

⁷A. Kamgar, P. Kneschaurek, W. Beinvoogl, and J. F.

- Koch, *Proceedings of the 12th International Conference on the Physics of Semiconductors, Stuttgart, 1974*, edited by M. H. Pilkuhn (Teubner, Leipzig, 1974), pp. 709–713.
- ⁸P. Kneschaurek, A Kamgar, and J. F. Koch, *Phys. Rev. B* **14**, 1610 (1976).
- ⁹W. P. Chen, Y. J. Chen, and E. Burstein, *Surf. Sci.* **58**, 263 (1976).
- ¹⁰S. J. Allen, D. C. Tsui, and B. Vinter, *Solid State Commun.* **20**, 425 (1976).
- ¹¹M. Nakayama, *Solid State Commun.* **21**, 425 (1977).
- ¹²T. Ando, *Z. Phys. B* **26**, 263 (1977).
- ¹³A. L. Fetter and J. D. Walecka, *Quantum Theory of Many-Particle Systems* (McGraw-Hill, New York, 1971).
- ¹⁴S. Das Sarma, R. K. Kalia, M. Nakayama, and J. J. Quinn, *Phys. Rev. B* **19**, 6347 (1979).
- ¹⁵R. K. Kalia, G. Kawamoto, J. J. Quinn, and S. C. Ying, *Solid State Commun.* **34**, 423 (1980).
- ¹⁶B. I. Lundqvist, *Phys. Kondens. Mater.* **6**, 193 (1976); **6**, 206 (1967).
- ¹⁷A. W. Overhauser, *Phys. Rev. B* **3**, 1888 (1970).
- ¹⁸A. J. Glick, *Phys. Rev.* **129**, 1399 (1963).
- ¹⁹A Zangwill and P. Soven, *Phys. Rev. B* **21**, 1561 (1980).
- ²⁰S. Das Sarma, Ph.D. thesis, Brown University, 1979, unpublished.
- ²¹J. J. Quinn, G. Kawamoto, and B. D. McCombe, *Surf. Sci.* **73**, 190 (1978).